American Mineralogist, Volume 93, pages 154–157, 2008

Barioperovskite, $BaTiO_3$, a new mineral from the Benitoite Mine, California

Chi Ma* and George R. Rossman

Division of Geological and Planetary Sciences, California Institute of Technology, Pasadena, California 91125-2500, U.S.A.

Abstract

Barioperovskite, ideally $BaTiO_3$, is a new member of the perovskite group. It is found as micro- to nano-crystals in a host of amorphous material contained within hollow, tubular inclusions in benitoite from the Benitoite Mine, San Benito County, California, U.S.A. The mean chemical composition determined by electron-microprobe analysis is (wt%) BaO 65.46, TiO_2 34.57, SiO_2 0.89, sum 100.92. The empirical formula calculated on the basis of 3 O is $Ba_{0.97}Ti_{0.98}Si_{0.03}O_3$. Barioperovskite is orthorhombic, *Amm*2; a = 3.9874 Å, b = 5.6751 Å, c = 5.6901 Å, V = 128.76 Å^3, and Z = 2. The electron backscattered diffraction pattern is an excellent match to that of synthetic $BaTiO_3$ with the *Amm*2 structure. The strongest calculated X-ray powder diffraction lines from the synthetic $BaTiO_3$ data are [d in Å, (I), hkl] 4.018 (18) (011), 2.845 (30) (002), 2.830 (100) (111), 2.316(20) (102), 2.312 (23) (120), 2.009 (28) (022), 1.640 (17) (113), 1.637 (19) (131), 1.633 (18) (202), and 1.415 (15) (222). The mineral is named after its composition, a Ba-dominant member of the perovskite group.

Keywords: Barioperovskite, new mineral, barium titanate, perovskite group, Benitoite Mine, $BaTiO_3$, $BaTi_2O_5$, $BaTi_3O_7$

Introduction

During our detailed microanalytical characterization of a polished benitoite crystal that we use as a primary electron-microprobe standard, we found micro- to submicro-inclusions of $BaTiO_3$, a new perovskite phase. Electron-microprobe, scanning electron microscope, electron backscatter diffraction, and Raman analyses have been used to characterize its composition and structure. Synthetic $BaTiO_3$ is well studied in the field of material science. Ultrafine particles of barium titanate were previously reported to occur in the matrix of the Allende meteorite (Tanaka and Okumura 1977), but due to their small size, their chemistry was not well defined and their crystal structure was not determined. Here, we document the occurrence of $BaTiO_3$ as a natural terrestrial phase.

The mineral is named for its composition, a Ba-dominant member of the perovskite group. The mineral and the mineral name have been approved by the Commission on New Minerals, Nomenclature and Classification (CNMNC) of the International Mineralogical Association (proposal IMA 2006-040). The holotype specimens of barioperovskite consisting of a polished crystal with three tubular inclusions have been removed from our electron microprobe standard block (P1014) and were deposited at the Smithsonian Institution's National Museum of Natural History, registration number NMNH 174513.

Occurrence

The mineral occurs in the Benitoite Mine (formerly the Dallas Gem Mine), near Santa Rita Peak, New Idria District, San Benito Mountains, San Benito County, California, U.S.A. (Wise and Gill 1977). At this mine, benitoite is found in natrolite veins in blueschist bodies within serpentinite. It is associated with neptunite, joaquinite-(Ce), jonesite, and djurleite, among others. A transparent, light blue benitoite ($BaTiSi_3O_9$) crystal from this locality was ground and polished to a flat surface for use as a standard for electron-microprobe analysis in our laboratory. The crystal contains four hollow, tubular inclusions, three of which are now exposed at the polished surface of the crystal (Fig. 1). The inclusions are sub-parallel to each other, but are not aligned with the principal crystallographic axes but, instead, run approximately parallel to [0 1 $\bar{1}$ $\bar{1}$] as determined from the electron backscatter diffraction pattern of the host crystal. Barioperovskite occurs as a component of the tubular inclusions. The size of the barioperovskite crystals, a few micrometers to sub-micrometer, required microanalytical methods to further characterize the phase.

Experimental details

Backscattered electron (BSE) images were obtained both with a LEO 1550VP field emission SEM and a JEOL 8200 electron microprobe. Quantitative elemental micro-analyses were conducted with the JEOL 8200 electron microprobe operated at 15 kV and 10 nA in a focused beam mode using the Probe for Windows software. Standards for the analysis were TiO_2 (Ti$K\alpha$) and benitoite (Ba$L\alpha$, Si$K\alpha$). Analyses were processed with the CITZAF correction procedure (Armstrong 1995).

Single-crystal electron backscatter diffraction (EBSD) analyses at a sub-micrometer scale were preformed using an HKL EBSD system on the LEO 1550VP scanning electron microscope, operated at 20 kV and 1 nA in a focused beam with a 70° tilted stage. The EBSD system was calibrated using a single-crystal silicon standard. The structure was determined and cell constants were obtained by matching the experimental EBSD pattern with the ICSD $BaTiO_3$, $BaTi_2O_5$, fresnoite, and benitoite structures.

Raman spectroscopic micro-analysis was carried out using a Renishaw M1000 micro-Raman spectrometer system on domains of the sample in polished section previously identified as $BaTiO_3$ crystals through BSE imaging and EBSD analysis. Approximately 1.4 mW of 514.5 nm laser illumination (at the sample) focused with a 100× objective lens provided satisfactory spectra. The spot size was about 2 μm. Peak positions were calibrated against a silicon standard. A dual-wedge polarization scrambler was used in the laser beam for all spectra to minimize the effects of polarization.

* E-mail: chi@gps.caltech.edu

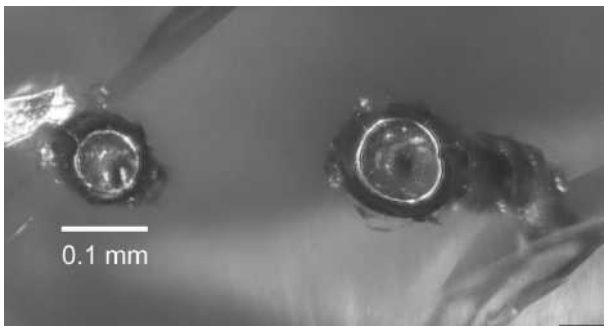

Figure 1. Photomicrograph of two hollow inclusions exposed at the surface of a polished crystal of benitoite. The left inclusion, which contains the *barioperovskite*, consists of a hollow core about 60 µm in diameter with a darker rim of mixed crystalline and amorphous material that ranges in thickness from 9 to 52 µm. The white ring at the immediate edge of the hollow core is an artifact from reflected light of the ring-illuminator used to illuminate the sample.

Results

Physical properties

Barioperovskite crystals were first recognized by their strong backscattered electron intensity in the scanning electron microscope (Fig. 2). They occur as individual, irregular grains, 1–10 µm, and tabular (at times, approaching dendritic) crystals usually <1 µm wide and 6–8 µm long. The physical appearance of the tabular crystals suggests that they may be part of a larger, partly hidden, dendritic structure. This suggestion is re-enforced by the EBSD patterns on several adjacent tabular crystals that indicate that the adjacent crystals have the same crystallographic orientation. No obvious crystal forms were observed. There was no visual indication of twinning and no indication of twinning in the EBSD patterns.

Color, refractive indices, optic sign, streak, luster, hardness, tenacity, cleavage, fracture, and density could not be determined because of the small grain size. There is no evidence of fluorescence under long-wave or short-wave ultraviolet radiation that could be seen above the fluorescence of the host benitoite. Cathodoluminescence was not observed under the SEM.

Chemical composition

BSE imaging and electron-probe analysis show that one tubular inclusion found in the benitoite crystal (Fig. 2) contains micrometer-sized crystals with an ideal chemical composition of $BaTiO_3$. Nine chemical analyses (Table 1) were carried out by means of an electron microprobe (wavelength-dispersive spectrometry mode, 15 kV, 10 nA, beam focused to a nominal 150 nm spot). No other elements with atomic number greater than 4 were detected. The analysis shows that these crystals have an empirical formula $Ba_{0.969}Ti_{0.982}Si_{0.034}O_3$. H_2O and CO_2 are absent (Raman spectrum). Because the crystals are naturally embedded in a barium titanium silicate matrix, some (if not all) of the silicon counts in the analysis are likely from excitation of the adjacent and underlying matrix. The empirical formula (based on three O apfu) is $Ba_{0.969}Ti_{0.982}Si_{0.034}O_3$. The simplified formula is $BaTiO_3$, which requires: BaO 65.74, TiO_2 34.26, Total 100.00 wt%. Nano-crystals of this $BaTiO_3$ phase also occur in the benitoite crystal within a third inclusion (Fig. 2c) that is not illustrated in Figure 1.

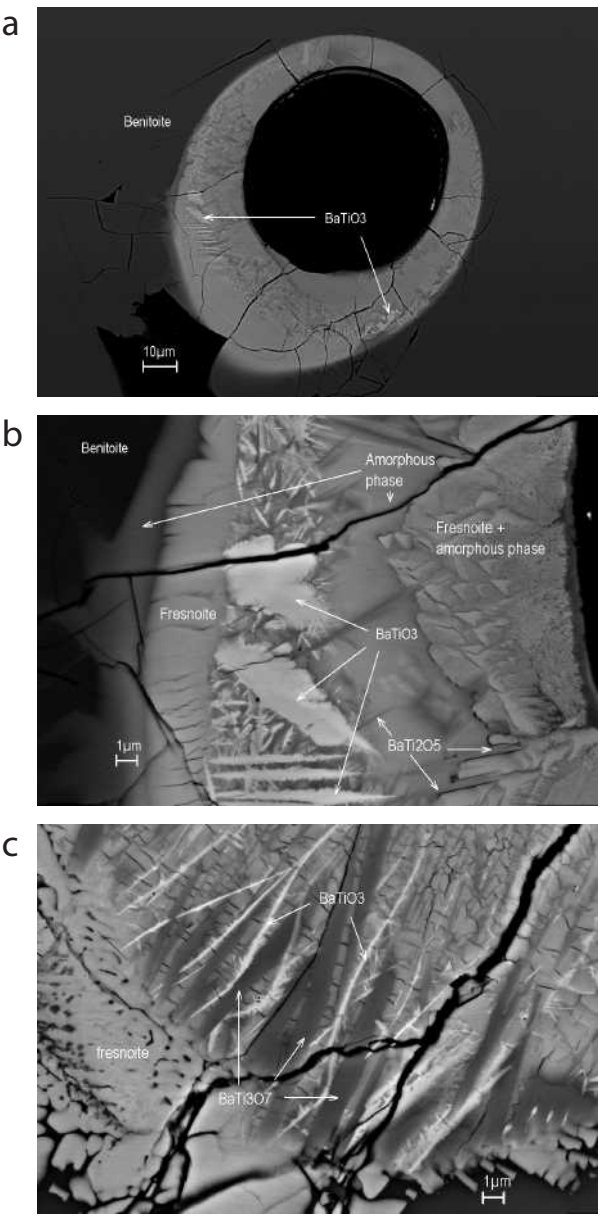

Figure 2. (**a**) BSE image of the 60 µm wide, tubular inclusion on the left side of Figure 1. It contains a hollow core surrounded by a rim of amorphous and crystalline phases. (**b**) Enlarged BSE image showing one area where $BaTiO_3$ micro- to nano-crystals occur in this tubular inclusion, along with $BaTi_2O_5$ and fresnoite. (**c**) BSE image showing one area where $BaTiO_3$ nano-crystals occur in the third inclusion (not shown in Fig. 1), along with $BaTi_3O_7$ and fresnoite.

Raman spectra

Raman micro-analyses show that the spectrum of the barioperovskite is similar to that of synthetic $BaTiO_3$, as shown in Figure 3, but that the Raman modes are broader than that of the single-crystal reference. The spectrum of no other Ba-titanite, Ba-titanosilicate, or Ba-silicate that we investigated came close

to resembling the pattern of barioperovskite. The Raman spectra of representative excluded candidate phases also appear in Figure 3. In addition to the broad features of barioperovskite, possible weak features of benitoite can be seen at about 575 and 535 cm^{-1} in our pattern as well as possible weak features from the adjacent phases.

Additional phases

Fresnoite ($Ba_2TiSi_2O_8$) is present in all tubular inclusions as shown by electron-microprobe analysis, the Raman spectrum, and the EBSD pattern. In all three tubular inclusions, we have regions that give EBSD and Raman patterns that match fresnoite. Much of this material in these regions is sub-micrometer in size and is too small to fill the beam of the electron microprobe. As such, the electron-microprobe analysis deviates significantly from the ideal fresnoite composition. One of regions (the widest) that gives an excellent EBSD fresnoite pattern shows a significant excess of Ti in the microprobe analysis. We do not know if the Ti excess is the actual composition of the inclusion, or if it is from unwanted electron beam excitation of nearby components.

An additional component that is EBSD-amorphous and Raman-amorphous occurs in all three tubular inclusions and is generally in contact with the barioperovskite and fresnoite. The electron-microprobe analysis of the amorphous material is relatively homogeneous within a single tubular inclusion, but varies from one inclusion to another, as shown in Table 2. No benitoite was found within contents of the tubular inclusions.

Barioperovskite occurs in two of the three tubular inclusions in benitoite. The inclusions are currently hollow tubes of 60–100 μm width whose interiors are partly coated with a mixture of crystalline materials and material that is EBSD- and Raman-amorphous (Fig. 2a). The $BaTiO_3$ is found as discrete crystallites up to 10 μm wide in this coating (Fig. 2b).

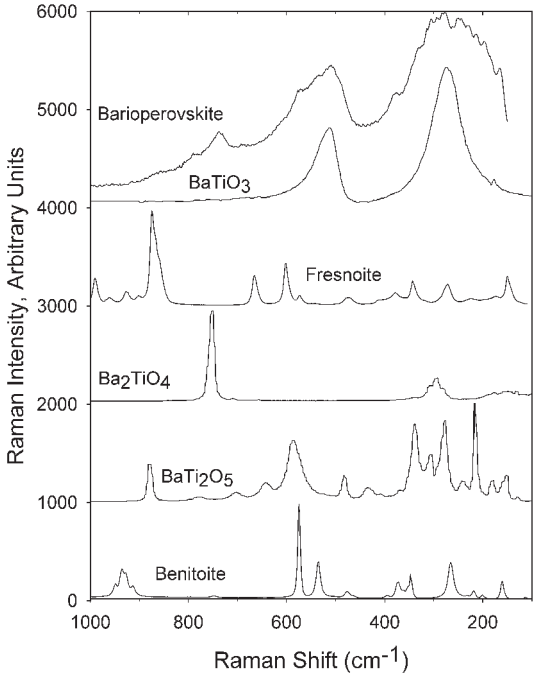

FIGURE 3. The Raman spectrum of barioperovskite (the upper, larger micro-crystal in Fig. 2b) compared to a synthetic $BaTiO_3$ from Jiang et al. (1996), and the candidate phases that might be expected in the inclusions in benitoite. Spectra are vertically offset for clarity.

Two more new Ba-titanate phases ($BaTi_2O_5$, $BaTi_3O_7$) were discovered at sub-micrometer to nanometer scales, along with barioperovskite and fresnoite within the amorphous materials in two inclusions. $BaTi_2O_5$ crystals were recognized by their lath shapes in the SEM images (Fig. 2b). They occur as individual, euhedral grains, 100 × 200 nm to 500 nm × 5 μm. The mean chemical composition of $BaTi_2O_5$ determined by electron-microprobe analysis on the largest crystals is (wt%) BaO 50.22, TiO_2 43.63, SiO_2 7.77, sum 101.62. The empirical formula calculated on the basis of 5 O is $Ba_{0.98}Ti_{1.63}Si_{0.39}O_5$. Its electron backscattered diffraction pattern is not a good match to that of synthetic $BaTi_2O_5$ with *C*2 structure, which may be due to Si substitution in the structure. Raman micro-analyses show that the spectrum of $BaTi_2O_5$ is not close to that of synthetic $BaTi_2O_5$, and it is also mixed with the spectrum of nearby phases.

Crystals of $BaTi_3O_7$ are lath-shaped, separate, 300 × 900 nm to 1 × 8 μm (Fig. 2c). The chemical composition of $BaTi_3O_7$ on the largest crystal is (wt%) BaO 40.81, TiO_2 59.53, SiO_2 0.51, sum 100.85. The empirical formula calculated on the basis of 7 O is $Ba_{1.05}Ti_{2.94}Si_{0.03}O_7$. Its EBSD pattern implies a low-symmetry structure. It was not indexed because the synthetic $BaTi_3O_7$ structure is unknown. The Raman modes of the $BaTi_3O_7$ are very broad and contaminated by nearby phases.

Both the $BaTi_2O_5$ and $BaTi_3O_7$ phases have been discussed in the material science literature (Kimura et al. 2003; Lu and Hong 2003), but $BaTi_3O_7$ has not been fully characterized. We were not able to determine the crystal structures of either phase based on their EBSD and Raman data because of their small grain size in the benitoite inclusions.

CRYSTALLOGRAPHY

Electron diffraction patterns

EBSD patterns of barioperovskite were matched against all the structural variants ($Pm\bar{3}m$, $P4mm$, $Amm2$, $R3m$) of synthetic $BaTiO_3$ reported in Kim et al. (2004), Aoyagi et al. (2002), Kwei et al. (1993), Waesche et al. (1981), and Megaw (1962); the patterns also were compared with the structures of $BaTi_2O_5$, benitoite, and fresnoite. The patterns were indexed to give a best fit based on $Amm2$ $BaTiO_3$ structure (Fig. 4) from Kwei et al. (1993), showing a = 3.9874 Å, b = 5.6751 Å, and c = 5.6901 Å. The calculated density is 5.91 g/cm^3 using the empirical formula and the cell constants from Kwei et al. (1993).

TABLE 1. Electron microprobe analysis results of barioperovskite

Constituent	wt%	Range	Stand. dev.
BaO	65.46	64.90–66.12	(41)
TiO_2	34.57	34.07–35.09	(32)
SiO_2	0.89	0.60–1.33	(27)
Total	100.92		

TABLE 2. Electron microprobe analysis results of amorphous phases

wt%	Inclusion 1*	Inclusion 2	Inclusion 3*
n	9	12	15
BaO	46.69(0.96)	48.37(1.58)	52.51(0.82)
TiO_2	16.61(0.89)	31.35(1.84)	29.27(1.73)
SiO_2	37.12(0.17)	21.09(1.81)	19.19(1.61)
Total	100.42	100.81	100.97

* Barioperovskite occurs in the two inclusions.

The $BaTiO_3$ crystals studied by electron backscatter diffraction are too small for single-crystal XRD study. The EBSD pattern (Fig. 4), determined in the SEM, was an excellent match to the computed EBSD pattern and cell parameters of synthetic $BaTiO_3$ (ICSD collection code 073641, PDF 81-2200) from Kwei et al. (1993). No errors are stated because the cell parameters are taken directly from the data of the matching $BaTiO_3$ phase in Kwei et al. (1993). The *a*:*b*:*c* ratio calculated from the unit-cell parameters is: 0.7026:1:1.0026. The crystals are orthorhombic with space group: *Amm*2; a = 3.9874 Å, b = 5.6751 Å, c = 5.6901 Å, V = 128.76 Å^3, and Z = 2. The XRD data used for this study were taken from PDF 81-2200, calculated from the ICSD structure (Kwei et al. 1993) using POWD-12^{++} (1997). The strongest calculated lines are [*d* in Å, (*I*), *hkl*] 4.018 (18) (011), 2.845 (30) (002), 2.830 (100) (111), 2.316(20) (102), 2.312 (23) (120), 2.009 (28) (022), 1.640 (17) (113), 1.637 (19) (131), 1.633 (18) (202), 1.415 (15) (222).

Discussion

The precursors of barioperovskite are believed to have formed under the same conditions as the associated benitoite. Benitoite is believed to form at a temperature below 95 °C (Wise and Gill 1977). We speculate that the Ba-titanate phases formed in a gel within the tubular inclusions. Support for this concept come from what appear to be late-stage shrinkage cracks that split $BaTiO_3$ and the remaining amorphous material within the tubular inclusions. Although it is possible that the $BaTiO_3$ formed at the time of benitoite crystallization, we think that it is more likely that it slowly crystallized in the amorphous material at a later time.

$BaTiO_3$ is a well-known and well-studied synthetic phase. It is widely used commercially because it has interesting ferroelectric, piezoelectric, and pyroelectric properties as well as useful non-linear optical properties and dielectric properties. At high temperature, $BaTiO_3$ has the cubic perovskite structure. $BaTiO_3$ undergoes three phase transformations with decreasing temperature. At ambient pressure, the compound is $Pm\bar{3}m$ cubic at high temperature, transforms to *P*4*mm* at 393 K, then to *Amm*2 at 278 K and finally to a *R*3*m* below 183 K (Kwei et al. 1993). Although it is generally believed that benitoite formed at a comparatively low temperature, its estimated conditions of formation (Wise and Gill 1977) are at higher temperatures than the transition temperature of $BaTiO_3$ from tetragonal to orthorhombic. The occurrence of the *Amm*2 polymorph in the inclusions in the natural sample suggests that the minor amount of Si found in the analysis may be incorporated in the structure of barioperovskite and that it contributes to the stability of the *Amm*2 polymorph at temperatures above 278 K.

As a follow up to the observations of Tanaka and Okumura (1977), we also carefully examined under the SEM several sections prepared from one Allende meteorite specimen in the Caltech collection but did not find any Ba-titanate phase. It is apparent that the Allende meteorite varies very much from one specimen to the other. Likewise, the tubular inclusions that contain barioperovskite are uncommon in benitoite. In addition to the three tubular inclusions exposed at the polished surface of our benitoite crystal, one additional tubular inclusion is contained entirely within the crystal. This inclusion has not been studied by any of the analytical methods used to characterize the barioperovskite. Numerous other benitoite crystals have been examined under the optical microscope, but, to date, no additional tubular inclusions have been identified.

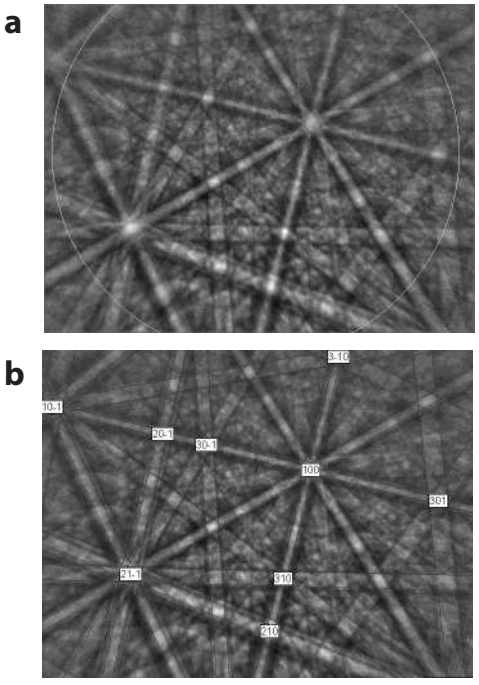

Figure 4. (**a**) EBSD pattern of the labeled $BaTiO_3$ crystal (upper one) in Figure 2b, (**b**) the pattern perfectly indexed with the $BaTiO_3$ *Amm*2 structure.

Acknowledgments

This work was funded, in part, through grant EAR-0337816 from the U.S. National Science Foundation and, in part, by the White Rose Foundation. The Caltech GPS Analytical Facility is supported, in part, by grant NSF EAR-0318518. We thank Anton Chakhmouradian and an anonymous reviewer for their constructive reviews.

References cited

Aoyagi, S., Kuroiwa, Y., Sawada, A., Yamashita, I., and Atake, T. (2002) Composite structure of $BaTiO_3$ nanoparticle investigated by SR X-ray diffraction. Journal of the Physical Society of Japan, 71, 1218–1221.

Armstrong, J.T. (1995) CITZAF: A package of correction programs for the quantitative electron microbeam X-ray analysis of thick polished materials, thin films, and particles. Microbeam Analysis, 4, 177–200.

Jiang, Y.J., Zeng, L.Z., Wang, R.P., Zhu, Y., and Liu, Y.L. (1996) Fundamental and second-order Raman spectra of $BaTiO_3$. Journal of Raman Spectroscopy, 27, 31–24.

Lu, C.-H. and Hong, H.-C. (2003) Effects of pH on formation and morphology of barium titanate powders prepared by coprecipitation process. British Ceramic Transactions, 102, 73–79.

Kim, Y.-I., Jung, J.K., and Ryu, K.-S. (2004) Structural study of nano $BaTiO_3$ powder by Rietveld refinement. Materials Research Bulletin, 39, 1045–1053.

Kimura, T., Goto, T., Yamane, H., Iwata, H., Kajiwara, T., and Akashi, T. (2003) A ferroelectric barium titanate, $BaTi_2O_5$. Acta Crystallographica, C59, 128–130.

Kwei, G.H., Lawson, A.C., Jr., Billinge, S.J.L., and Cheong, S.-W. (1993) Structures of the ferroelectric phases of barium titanate. Journal of Physical Chemistry, 97, 2368–2377.

Megaw, H.D. (1962) Refinement of the structure of $BaTiO_3$ and other ferroelectrics. Acta Crystallographica, 15, 972–973.

Tanaka, T. and Okumura K. (1977) Ultrafine barium titanate particles in the Allende meteorite. Geochemical Journal, 11, 137–145.

Waesche, R., Denner, W., and Schulz, H. (1981) Influence of high hydrostatic pressure on the crystal structure of barium titanate ($BaTiO_3$). Materials Research Bulletin, 16, 497–500.

Wise, W.S. and Gill, R.H. (1977) Minerals of the Benitoite Gem Mine. Mineralogical Record, 8, 442–452.

Manuscript received March 16, 2007
Manuscript accepted September 11, 2007
Manuscript handled by Sergey Krivovichev